Formation of non-equilibrium solid phases in Fe-Nb multilayered films by ion irradiation

1998 J. Phys.: Condens. Matter 10 10805

(http://iopscience.iop.org/0953-8984/10/48/004)

J. Phys.: Condens. Matter **10** (1998) 10805–10813. Printed in the UK PII: S0953-8984(98)95588-6

Formation of non-equilibrium solid phases in Fe–Nb multilayered films by ion irradiation

C Lin, J B Liu, G W Yang and B X Liu

Department of Materials Science and Engineering, Tsinghua University, Beijing 100084, People's Republic of China

Received 6 July 1998, in final form 26 August 1998

Abstract. In the Fe–Nb system, amorphous alloy, metastable crystalline fcc and hexagonal phases were formed in Nb-rich multilayered films by room temperature 200 keV xenon ion mixing. A heat of formation diagram of the system was constructed based on Miedema's model and Alonso's calculation method, and the diagram gave a relevant interpretation for the observed phase formation. The formation of fcc metastable phase can be interpreted by a reverse martensitic transition of bcc–fcc. The amorphous and hexagonal phases are thought to form through a traditional nucleation and growth mechanism with an additional consideration of the irradiation effect, which kinetically hindered the formation of a complicated intermediate compound.

1. Introduction

The continuously growing need of new materials with unique properties for various applications has stimulated great interest in understanding of metastable materials in either crystalline or amorphous state. Ion beam mixing of multilayered films has been used extensively to study the formation of metastable alloy phases since the 1980s, as its effective cooling speed can be as high as 10^{14} K s^{-1} and the experimental parameters are easy to control [1, 2]. Up to now, more than 90 binary metal systems have been investigated and a great number of amorphous alloys and different structured metastable crystalline phases have so far been observed. The metastable crystalline phases are of supersaturated solid solution, hcp phase in hcp–bcc or fcc–bcc systems on the hcp-rich or fcc-rich side, fcc phase in hcp-based systems and fcc and hcp phases in some bcc-based systems [3].

In the previous studies [4], a two-step phase transformation of bcc $\rightarrow$ hcp $\rightarrow$ fcc was observed in the Fe–Nb system at alloy composition close to Nb. The transformation is diffusionless and undergoes through two consecutive steps, i.e., a shearing for the bcc–hcp and then a sliding for the hcp–fcc transitions. In this study, the detailed phase evolutions in ion irradiated Fe/Nb multilayered films were investigated, and an fcc and a hexagonal phase with enlarged lattice constants were obtained.

2. Experimental procedure

The Fe–Nb multilayered films with 10 layers were prepared by depositing alternately pure iron and niobium onto freshly cleaved NaCl single crystals at rate of about 0.1–0.2 nm per second in an e-gun evaporation system with a vacuum level on the order of 10^{-5} Pa. To

0953-8984/98/4810805+09$19.50

reduce the possible oxidation of the constituent metals, Ti was evaporated first and deposited onto a spare SiO_2 substrate to adsorb the residual oxygen in the vacuum system before depositing the multilayered samples. The total thickness of the films was about 50 nm, which matched the projected range (R_p) plus the projected range straggling (ΔR_p) of the irradiating ions, i.e. 200 keV xenon ions employed in this study. The thickness of each layer was controlled by an *in situ* quartz oscillator in the evaporator. The as-deposited Fe–Nb multilayered films were immediately moved into and stored in a dry vacuum chamber to avoid contamination before subject to ion irradiation. Energy dispersive spectroscopy (EDS) was employed to confirm the overall compositions of the as-deposited films and to determine the real compositions of the films after ion irradiation. The analysis error involved in EDS was less than 5%. Ion irradiation of the samples was conducted at room temperature (RT) with xenon ions to doses from 3×10^{14} to 5×10^{15} Xe^+ cm^{-2} in an implanter with a vacuum level better than 5×10^{-4} Pa. The ion current density was confined to be less than 1 μA cm^{-2} to minimize the beam heating effect. After irradiation, all the irradiated films were removed from the NaCl substrates in de-ionized water and put on Cu grids for transmission electron microscopy (TEM) examination and selected area diffraction (SAD) analysis to identify the resultant structure.

3. Results and discussion

The phase evolution in the Fe–Nb multilayered films upon RT 200 keV xenon ion irradiation is listed in table 1. It can be seen that the Fe in the as-deposited $Fe_{12}Nb_{88}$ and $Fe_{27}Nb_{73}$ films is in an amorphous state, while it is of crystalline structure in the $Fe_{34}Nb_{66}$ films. The thickness of Fe layers in these samples are about 0.9, 2.0 and 2.7 nm, respectively, which is believed to relate the structure in the as-deposited films. It is well known that there is a critical Fe thickness for the transformation from amorphous state to nanocrystalline structure, and a typical value of the critical thickness is about 2.3 nm [5]. As a result, the Fe layers would keep the amorphous state in the first two samples, as the thickness is smaller than the critical value, which is due to a misfit between the lattices of bcc Fe and of either the substrate or of the Nb. The Fe layers would change into crystalline structure in the third sample, as the layer thickness is greater than the critical value. However, the amorphous Fe layers would change into a crystalline structure if excess energy were transferred to the Fe atoms from the irradiation ions at a relative low irradiation dose, as shown in the table.

Table 1. Phase changes in the Fe–Nb multilayered films induced by room temperature 200 keV xenon ion mixing. (amor. stands for amorphous phase; fcc and hex. are three metastable phases.)

Dose ($\times 10^{14}$ Xe^+ cm^{-2})	$Fe_{12}Nb_{88}$	$Fe_{27}Nb_{73}$	$Fe_{34}Nb_{66}$
3	Nb+amor. Fe	Nb+amor. Fe	Nb+Fe
5	Nb+amor. Fe	Nb+amor. Fe	Nb+fcc
7	Nb+Fe	Nb+fcc	Nb+fcc
10	Nb+Fe	Nb+fcc	Nb+amor.
50	Nb+hex.	amor.+hex.	amor.+hex.

For the $Fe_{34}Nb_{66}$ films, firstly, an fcc phase with a lattice constant of 0.355 nm was observed together with a crystalline Nb at an irradiation dose of 5×10^{14} Xe^+ cm^{-2}. An amorphous phase was observed together with a crystalline Nb at an irradiation dose of 1×10^{15} Xe^+ cm^{-2}. Eventually, a hexagonal phase and an amorphous phase were observed

at an irradiation dose of 5×10^{15} Xe^+ cm^{-2}. These results can be summarized as follows:

$$Fe_{34}Nb_{66} \xrightarrow{5\times10^{14}} Nb + fcc \xrightarrow{1\times10^{15}} Nb + amor. \xrightarrow{5\times10^{15}} amor. + hex.$$

For the $Fe_{27}Nb_{73}$ films, the phase evolution was similar to that in the $Fe_{34}Nb_{66}$ films, but the fcc phase was formed at an irradiation dose of 7×10^{14} Xe^+ cm^{-2}. The phase evolution can be expressed by

$$Fe_{27}Nb_{73} \xrightarrow{7\times10^{14}} Nb + fcc \xrightarrow{5\times10^{15}} amor. + hex.$$

For the $Fe_{12}Nb_{88}$ films, neither fcc nor Fe–Nb amorphous solution phase was detected at any irradiation doses. Instead, only a hexagonal phase was observed at an irradiation dose of 5×10^{15} Xe^+ cm^{-2}

$$Fe_{12}Nb_{88} \xrightarrow{5\times10^{15}} Nb + hex.$$

The SAD patterns of the $Fe_{34}Nb_{66}$ films at various irradiation stages are shown in figure 1, and the corresponding indexing results are listed in tables 2–4, respectively. It is worthwhile mentioning that the diffraction lines of the observed metastable phases could not be matched with those Fe–Nb intermediate phases like FeNb, Fe_2Nb or Fe and Nb oxides listed in the documented ASTM cards. It is also believed that the possible Cl and Na atoms from the substrates did nothing to the observed phase formation. As mentioned above, for the designed thickness of the Fe–Nb multilayered films, i.e. $(R_p + \Delta R_p)$, the probabilities of recoiling events were minimized and thus only a trace amount of Na and Cl atoms were mixed into the films. Even if there were some Na and Cl atoms in the films, they would prefer to form NaCl crystals, as the binding energy of NaCl was the highest one compared with other possible compounds. Hydrogen was also a very minor impurity, since the films were stored in a dry vacuum chamber. Furthermore, it was found in previously studied metal–metal multilayered films by x-ray phonon spectrum (XPS) analysis that hydrogen appeared only in the very surface within 1 nm, which should have no detectable influence on the SAD patterns.

Table 2. Indexing results of the as-deposited $Fe_{34}Nb_{66}$ multilayered films. ($a_{Fe} = 0.275$ nm, $a_{Nb} = 0.341$ nm.)

$d_{experimental}$ (nm)	Fe(hkl)	Nb(hkl)
0.241		110
0.192	110	
0.140		211
0.137	200	
0.113	211	
0.097	220	

The next question is then what is the essential thermodynamics responsible for the phase formation and evolution in the Fe–Nb system. Generally, the Gibbs free energy of a phase can be calculated by $\Delta G = \Delta H - T\Delta S$, where ΔH and ΔS are the enthalpy and entropy of formation, respectively. The entropy usually plays only a secondary role in solid phase formation and is negligible. Following the well documented literature [6], the heat of formation of the equilibrium ordered phases can be easily calculated. We now discuss the calculation method for solid solution, metastable amorphous and crystalline phases. The formation enthalpy of a solid solution of transition metals consists of three terms

$$\Delta H^{ss} = \Delta H^{chemical} + \Delta H^{elastic} + \Delta H^{structural}$$

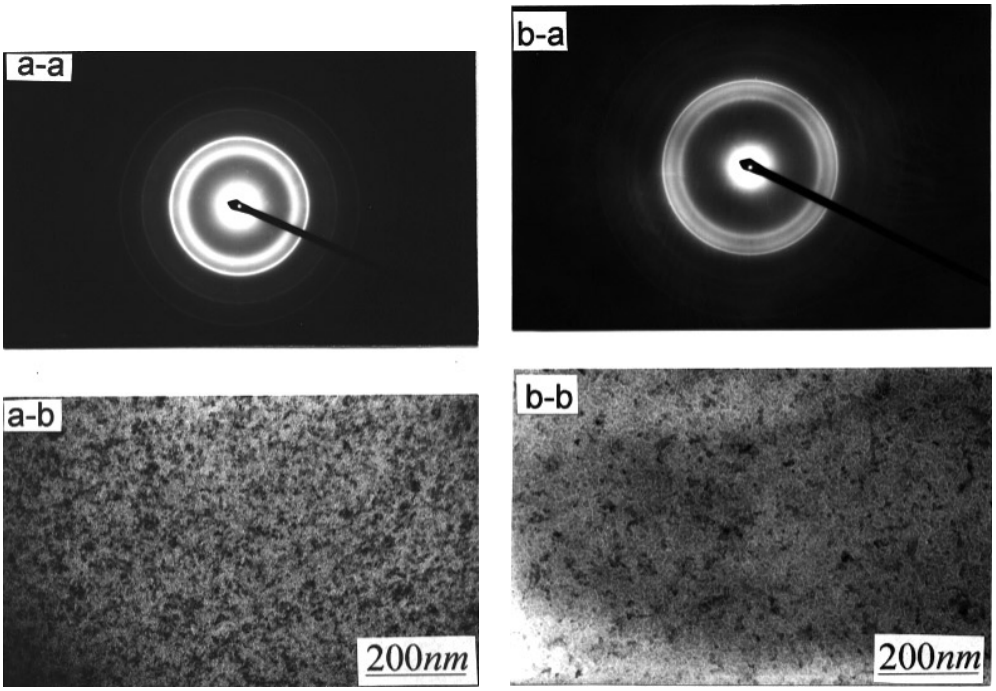

(a) (b)

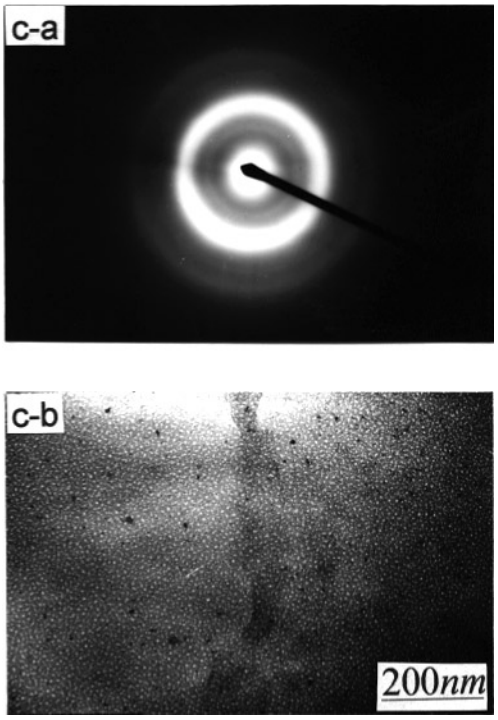

(c)

Figure 1. Selected area diffraction (SAD) patterns and corresponding bright-field images of the $Fe_{34}Nb_{66}$ multilayered films: (a-a) and (a-b) as deposited; (b-a) and (b-b) at an irradiation dose of 5×10^{14} Xe^{+} cm^{-2}; (c-a) and (c-b) at an irradiation dose of 5×10^{15} Xe^{+} cm^{-2}.

Table 3. Indexing results of the $Fe_{34}Nb_{66}$ multilayered films under 200 keV room temperature xenon ion mixing to an irradiation dose of 5×10^{14} Xe^+ cm^{-2}. (Fcc: $a = 0.355$ nm.)

$d_{experimental}$ (nm)	Intensity	Nb(hkl)	Fcc(hkl)	$d_{calculation}$ (nm)	$\lvert\Delta d\rvert$ (nm)
0.205	Strong		111	0.205	0.000
0.175	Strong		200	0.178	0.003
0.170	Very strong	200			
0.125	Medium		220	0.126	0.001
0.117	Medium	220			
0.108	Weak		311	0.107	0.001
0.103	Weak		222	0.102	0.001
0.095	Strong	222			
0.091	Weak		400	0.089	0.002
0.082	Medium	400			
0.079	Weak		331	0.081	0.002
0.075	Medium	402			

Table 4. Indexing results of the $Fe_{34}Nb_{66}$ multilayered films under 200 keV room temperature xenon ion mixing to an irradiation dose of 5×10^{15} Xe^+ cm^{-2}. ($a_{hex} = 0.364$ nm, $c_{hex} = 0.41$ nm.)

$d_{experimental}$ (nm)	Intensity	Hex.(hkl)	Amor.	$d_{calculation}$ (nm)	$\lvert\Delta d\rvert$ (nm)
0.315	Weak	100		0.315	0.000
0.205	Strong	002	halo nearby	0.205	0.000
0.186	Strong	110		0.182	0.004
0.144	Medium	201		0.147	0.003
0.121	Weak	210	halo nearby	0.119	0.002
0.111	Weak	211		0.114	0.003

which correspond to chemical, elastic and structural contributions, respectively. The chemical contribution, due to the electron redistribution generated at the contact surface between dissimilar atomic cells, is expressed as

$$\Delta H^{chemical} = X_A f_{AB} \Delta H^{interface}$$

where f_{AB} is a function which accounts for the degree to which an atom of A is surrounded by atoms of B, and is given by

$$f_{AB} = X_B^S[1 + \gamma(X_A^S X_B^S)]$$
$$X_B^S = \frac{X_B V_B^{2/3}}{X_A V_A^{2/3} + X_B V_B^{2/3}}$$

where γ is an empirical constant, and is used to describe the short-range order difference of solid solutions, amorphous phases and ordered compound, and is taken as 0, 5 and 8, respectively. $\Delta H^{interface}$ is the microscopic interfacial energy at zero temperature between the cells of dissimilar A and B, which can be calculated from:

$$\Delta H^{interface} = \frac{V_A^{2/3}}{(n_{WS}^{-1/3})_{av}}[-P(\Delta\varphi^*)^2 + Q(\Delta n_{WS}^{1/3})^2]$$

where $V^{2/3}$ is the atomic volume of the component A in the alloy, $(n_{WS}^{1/3})_{av}$ is the mean value of the electron density at the boundary of the Wigner–Seitz cell as derived for the pure elements in the metallic state $(n_{WS}^{1/3})_A$ and $(n_{WS}^{1/3})_B$, $\Delta\phi^*$ is the difference between ϕ_A^* and ϕ_B^*, i.e. the work function of pure metallic elements A and B; P and Q are constants determined empirically and had the values of 14.2 and 133.48, respectively. The elastic term, which is originated from atomic size mismatch, can be expressed as [7]:

$$\Delta H^{elastic} = X_A X_B [X_A \Delta H^{elastic}_{(B\,in\,A)} + X_B \Delta H^{elastic}_{(A\,in\,B)}]$$

where $\Delta H^{elastic}_{(i\,in\,j)}$ $(i, j = \mathrm{A}, \mathrm{B})$ is the elastic contribution to the formation enthalpy and can also be obtained from [6]. The structural term, reflecting the preference of the certain transition metals to crystallize in one of the main crystallographic structures bcc, fcc and hcp, is given by [6]:

$$\Delta H^{structure}_{(A\,in\,B)} = (Z_A - Z_B)\frac{\partial}{\partial Z}E_B(Z) + E_B(Z) - E_A(Z)$$

where $E(z)$ is the structural stability as a function of valence number Z per atom, which can also be found from [6]. The formation enthalpy of solid solution can be obtained by using the above equations.

The metastable crystalline phase can be considered to be compoundlike yet the occupancy of the constituent atoms is different from that in the completely ordered compound. The chemical term in the formation enthalpy can be expressed as [8]:

$$\Delta H(\eta) = \Delta H(1) + \{\Delta H(0) - \Delta H(1)\}(1 - \eta^2)$$

where $\Delta H(1)$ is the enthalpy of the compound, $\Delta H(0)$ is the chemical contribution to the enthalpy of the solid solution and is thus equal to $\Delta H^{chemical}$ of the solid solution. η is a long-range-order parameter, $\eta = 1$ and 0 are for completely ordered compound and solid solution, respectively. It is well known that the elastic contribution to formation enthalpy of the compound can be neglected, as the lattice distortion caused by the atomic size mismatch of the two constituent metals can be relaxed down to a minimum by the ordered arrangement of the atoms. The elastic contribution for a metastable phase can therefore be divided into two categories [9]: (1) if a metastable phase formed at a composition near an equilibrium compound, the elastic term of the metastable phase cannot be neglected, as the structure and the atomic arrangement are different from that of the equilibrium compound and thus cannot relax the lattice distortion to a minimum. (2) If a metastable phase is formed near an eutectic point, in which no corresponding equilibrium compound exists, the elastic term is negligible as the ordered arrangement of the atoms can relax the lattice distortion to a minimum. In our case, the elastic term is negligible, for the compositions of the metastable phases are in the two phase regions. The structural term of the metastable crystalline phase can also be neglected as in the case of compound, for it has only a minor effect on the formation enthalpy for the compoundlike metastable phase in the system.

According to Alonso *et al* the formation enthalpy of metastable amorphous phase is given by [10]:

$$\Delta H^{amor} = \Delta H^{chemical} + X_A \Delta H_A^{l-s} + X_B \Delta H_B^{l-s}$$

where ΔH^{l-s} is the difference in enthalpy between the undercooled liquid and the crystalline phases of the pure elements and can be calculated from

$$\Delta H_i^{l-s} = \frac{2T(T_{m,i} - T)\Delta H_i^{fuse}}{T_{m,i}(T_{m,i} + T)}$$

Table 5. Values of the parameters used in calculating the formation heat diagram of the Fe–Nb system.

	Fe	Nb	Metastable amor.	Metastable crystalline	Solid solution
Melting point T_m (K)	1808	2741			
ΔH_{l-s}^{fuse} (kJ mol^{-1})	13.8	30			
$V^{2/3}$ (cm^2)	3.69	4.89			
ϕ (volt)	4.93	4.05			
$n_{WS}^{1/3}$ (density unit)$^{1/3}$	1.77	1.64			
γ			5	8	0
$\Delta H_{(Fe\,in\,Nb)}^{elastic}$ (kJ mol^{-1})					31
$\Delta H_{(Nb\,in\,Fe)}^{elastic}$ (kJ mol^{-1})					58

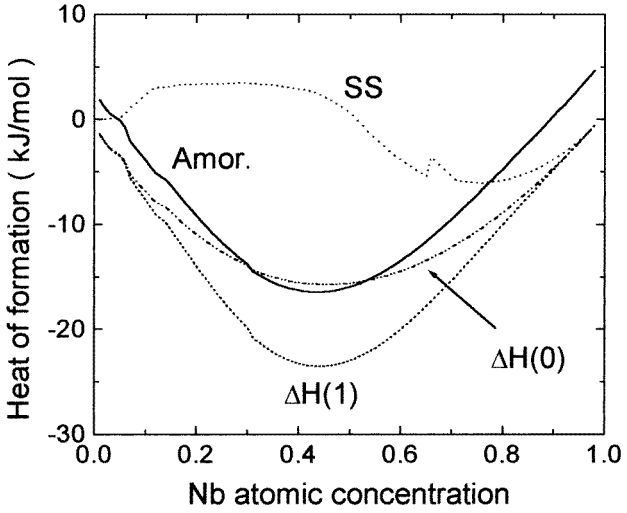

Figure 2. The calculated heat of formation diagram of the Fe–Nb system at $T = 298$ K. (Amor. stands for amorphous phase; ss stands for solid solution; $\Delta H(1)$ stands for the formation enthalpy for compound; $\Delta H(0)$ stands for the chemical term of the formation enthalpy for solid solution; the formation enthalpy of the metastable crystalline phase is located in the band between $\Delta H(1)$ and $\Delta H(0)$).

where $i = \mathrm{A}, \mathrm{B}$, ΔH^{fuse} is the heat of fusion and T_m is the melting point of the constituent element i, and T is the reference temperature with a value of 298 K here.

Accordingly, the formation enthalpy of the solid solution, amorphous phase and the metastable crystalline phases were calculated using the parameters listed in table 5 and the results are shown in figure 2. It should be noted that η is difficult to calculate, however, the enthalpy of the metastable phase should be located in a band between $\Delta H(0)$ and $\Delta H(1)$ shown in the figure. From the figure, it can be seen that the formation enthalpy curve of the amorphous is merged into the formation enthalpy band of the metastable crystalline phase in the vicinity of the equiatomic concentration, suggesting a large possibility for the co-existence of an amorphous and a metastable crystalline phase.

How the metastable crystalline phases were formed under the restricted kinetic conditions in ion irradiation and what is the structural relationship between the newly

formed metastable phases and the parent constituent metals. It is generally recognized that ion irradiation is a non-equilibrium process and can be divided into two phases, collision cascade and relaxation phases. When an irradiation ion with an energy E_1 collides with the target atoms, a target atom will receive an energy E_2. If E_2 exceeds a threshold energy E_d, that atom will be knocked out from its original lattice site and a vacancy is created. The knocked out atom will trigger secondary collision, and so on and forth, thus inducing an atomic collision cascade in the target materials. In this phase, the point defects are created and the average kinetic energy per atom in the cascade exceeds the average potential energy. The collision cascade is responsible for the intermixing of the metal atoms in the multilayered films. If the irradiation dose reaches an adequate value, the constituent atoms mix uniformly and later the target in a high energy state will relax towards the equilibrium state directed by the thermodynamics. However, whether the mixture can reach the equilibrium state depends on the temperature and time conditions available during the relaxation phase. Generally, the relaxation phase is very short, and thus the mixture cannot reach the equilibrium state in most cases; instead, it would stop at some intermediate states corresponding to metastable crystalline or amorphous phase. Since the phase formation by ion irradiation is a solid–solid transformation, there should be a structural compatibility between the newly formed metastable crystalline phases and the parent metals. In our case, the fcc phase can be formed from the Fe matrix. Generally, the direct transformation from bcc to fcc structure is a little difficult. In our previous studies, however, a two-step transformation mechanism of bcc $\rightarrow$ hcp $\rightarrow$ fcc (reverse martensitic mode) was proposed and it can be completed relatively easily. From a crystallographic point of view, the first step of bcc $\rightarrow$ hcp can be fulfilled by a shearing process, during which the (111) bcc acts as the habit plane, while $[\bar{1}1\bar{1}]_{bcc}([2\bar{1}0]_{hcp})$ acted as the shearing axis. The shearing process results in a relationship of $a_{hcp} = (\sqrt{3}/2)a_{bcc}$ and $c_{hcp} = \sqrt{2}a_{bcc}$. The hcp $\rightarrow$ fcc can be realized by a sliding on the $(002)_{hcp}$ plane along various $\langle 1\bar{1}0\rangle_{hcp}$ directions by a vector of $1/3\langle 1\bar{1}0\rangle_{hcp}$. The orientation relationship is $[11\bar{2}]_{fcc}//[1\bar{1}0]_{hcp}$, which results in a lattice parameter relationship as $a_{fcc} = \sqrt{2}\ a_{hcp}$ and $a_{fcc} = (\sqrt{3}/2)\ c_{hcp}$. Thus the lattice constant of the fcc can be deduced to be $a_{fcc} = (\sqrt{6}/2)\ a_{bcc}$. Using the lattice constant of Fe (0.275 nm), the lattice constant of the fcc phase can be calculated to be 0.336 nm. Comparing with our experimental result that the lattice constant was 0.355 nm, the difference between the experimental value and the deduced one is about 5%.

The hexagonal and amorphous phases were thought to form through a traditional nucleation and growth mechanism. It should be noted that in the equilibrium phase diagram of the Fe–Nb system, there is a μ phase containing 47–49 at% of Fe. The μ phase is commonly considered to be difficult to form by ion irradiation [1], as it has large lattice constants $a = 0.4928$ and $c = 2.683$ nm, respectively, and contains many atoms (13 atoms) in an unit cell. To form such a complicated phase, long-range diffusion of atoms is necessary, yet it can not proceed in ion irradiation, a process far from equilibrium. Though the energy deposited by the incident ions keeps driving thermodynamically the films to transform into the equilibrium μ phase having the lowest energy, the relaxation phase in the process of ion irradiation lasts only for 10^{-10}–10^{-9} seconds, preventing the μ phase from nucleating and growing. The restricted kinetic condition available during ion irradiation is thus favourable for the formation of either an amorphous or a simple structured crystalline phase. That is why a mixture of amorphous and hexagonal phases in the $Fe_{27}Nb_{73}$ and $Fe_{34}N_{66}$ films and a mixture of crystalline Nb and hexagonal phases in $Fe_{12}Nb_{88}$ films were observed, respectively.

4. Conclusion

(1) The formation of amorphous, metastable fcc and hexagonal crystalline phase in the Fe–Nb system on the Nb-rich side was observed by 200 keV xenon ion mixing at room temperature.
(2) The heat of formation diagram of the Fe–Nb system was established by calculating the formation enthalpy curves of the phases, including the amorphous, terminal solid solution and metastable crystalline ones and the diagram can give a reasonable interpretation for the phase formation.
(3) The ion irradiation effects were considered to hinder kinetically the formation of the equilibrium μ phase of complicated structure in the Fe–Nb system and thus to favour the formation of metastable phases.

Acknowledgments

The authors are grateful to the researchers of the Transmission Electron Microscopy Laboratory of Peking University and the Analysis Center and Materials Research Institute of Tsinghua University for their help. Financial aid from the National Natural Science Foundation of China is also acknowledged.

References

[1] Hung L S, Mastasi M, Gyulai J and Mayer J W 1983 *Appl. Phys. Lett.* **42** 627
[2] Liu B X, Johnson W L, Nicolet M A and Lau S S 1983 *Appl. Phys. Lett.* **42** 45
[3] Liu B X and Jin O 1997 *Phys. Status Solidi* a **161** 3
[4] Zhang Z J and Liu B X 1994 *J. Appl. Phys.* **75** 4948
[5] Landes J, Sauer Ch, Kabius B and Zinn W 1991 *Phys. Rev.* B **44** 8343
[6] Miedema A R, Niessen A K, de Boer F R, Boom R and Mattens W C M 1989 *Cohesion in Metals: Transition Metal Alloys* (Amsterdam: North-Holland)
[7] Lopez J M and Alonso J A 1984 *Phys. Status Solidi* a **85** 423
[8] Bakker H, Zhou G F and Yang H 1995 *Prog. Mater. Sci.* **39** 159
[9] Zhang Z J, Jin O and Liu B X 1995 *Phys. Rev.* B **51** 8076
[10] Alonso J A, Gallego L J and Lopez J M 1988 *Phil. Mag.* A **58** 79